



Exploration of Trigonal Patch Antenna Characteristics with the Impact of 2D Photonic Crystal of Various Air Hole Shapes

Sathish Kumar Danasegaran¹ · Elizabeth Caroline Britto¹ · Susan Christina Xavier²

Received: 26 December 2020 / Accepted: 16 June 2021 / Published online: 28 June 2021
© The Minerals, Metals & Materials Society 2021

Abstract

The terahertz (THz) band contributes significantly to high-speed data rates in short-distance communication. This article proposes a unique design of the trigonal microstrip patch antenna on photonic crystal (PhC) substrate in THz communication. The PhC design structure employs unique air-hole shapes such as L, H, T, I and upturned L instead of regular periodic latitude holes. The proposed antenna substrate uses Rogers RO4350 material, which helps to attain high gain and almost negligible return loss at THz frequency. The antenna performance is investigated with different PhC air-hole shapes. The I-shaped air-hole PhC antenna offered a meager return loss of -58.99 dB with a high gain of 9.1 dB and directivity of 10.7 dBi. The CST studio tool helps to simulate the parametric analysis of the proposed antenna design. This compact PhC antenna structure is apt for wireless communication, particularly in THz applications.

Keywords Trigonal patch antenna · photonic crystal · photonic bandgap · square lattice · terahertz frequency

Introduction

In recent years, the necessity of telecommunications is increasing fast and the technology requires the high-speed transmission of data. More researchers are trying to find out how to increase the communication speed in the range of terabytes per second (Tbps) by numerous techniques and methods in THz antenna. The THz radiation waves or waves of the submillimeter are occupied between 0.03 and 3 mm in the International Telecommunications Union (ITU). The frequency emission in the THz band ranges from 0.1 to 10 THz. THz communication helps to gain effective transmission at the rate of 1 Tbps. Various THz applications include telecommunication,¹ satellite links, security applications at airports, explosive detection, material identification, detection of metallic and nonmetallic contamination.² THz imaging includes detection of liver cancer, breast tumors,

deoxyribonucleic acid (DNA) sensing,³ spectroscopy and various health monitoring systems.⁴

In communication systems, the microstrip patch antenna is of interest due to its merits of compact,⁵ conformability and easy placement on a printed circuit board. It plays a significant role in satellite and missile applications.⁶ The microstrip patches are used in various shapes,^{7,8} such as square, rectangle, circle, dipole, triangular, elliptical. This paper designs the trigonal patch antenna since it reduces the antenna size, radiation loss and increases directivity value. The antenna design incorporates various feeding methods microstrip line, coaxial probe, aperture coupling and sector wavelength. This paper adopts the microstrip line feed technique because it is very much ingenious compared to other feeds. One of the demerits in the microstrip patch antenna is that more power radiated towards the substrate than the air-side.

PhC and metamaterials are two different artificial materials used in the patch antenna design.⁹ In PhC structure, atoms and lattice constant are similar to the wavelength of $a = \lambda$ and the diffraction has created the band gap. However, in metamaterials, the non-natural atoms and lattice constant have to be far smaller than the wavelength $a \ll \lambda$, so diffraction would not occur in this condition. Also, metamaterials reveal a negative refractive index value.^{10–13} The drawbacks of a metamaterial antenna are low gain, more electrical

✉ Sathish Kumar Danasegaran
dsathish@ifet.ac.in

¹ Electronics and Communication Engineering Department, IFET College of Engineering, Villupuram, Tamil Nadu, India

² Electronics and Communication Engineering Department, MAM College of Engineering, Trichy, Tamil Nadu, India

losses and limited operational bandwidth. Hence, PhC is different from metamaterials, and PhC is considered in this paper for the antenna design.

PhC provides a solution to this complexity when employed as a substrate. PhC helps to restrict and handle light and it reduces the surface waves. PhC with a photonic band gap (PBG) precludes light propagating in some directions with described frequencies in a low loss periodic dielectric medium. So far, many researchers designed only the circular air-hole^{6,8,10–12,14–16} PhC antennas and analyzed the antenna radiation characteristics. This paper delivers the novel air-hole shapes in a PhC substrate instead of the regular circular holes. The 2D PhC design is implanting the square array of different shapes of air-hole in a dielectric substrate.

This paper aims to design the PhC substrate for various hole shapes such as L, H, I, T and inverted L. With the assistance of CST microwave studio, the proposed five structures are designed and simulated. The antenna performances of all structures are compared with the conventional antenna. The 2D PhC helps to enhance the bandwidth and gain of the TMPA in THz frequencies. The arrangement of this paper, sect. “Principle of Light Propagation in PhC” describes the principle of light propagation in 2D PhC and sect. “Proposed Design” explains the proposed design and simulation output. Section “Discussion of Simulated Result” discusses the simulated output and sect. “Conclusion” states the conclusion.

Principle of Light Propagation in PhC

In periodic structures, electromagnetic wave propagation leads to pseudo-gaps due to the dispersion relation. Inside the pseudogap, the propagating waves have frequencies only for some k-points and forbid other k-points. The complete ‘band gap’ is acquired when the extension of the forbidden region covers all the directions of propagation related to dispersion. With the support of the PBG effect, the electromagnetic waves are trapped and become unable to radiate in any direction. It can hinder the spread along the axis of the substrate side, so it diminishes the absorption of electromagnetic waves through an antenna substrate and raises the reflection of electromagnetic waves towards space. All these merits lead to gain improvement and reduce the return loss of the antenna. This restraint helps to improve the antenna efficiency^{14–21} and decreases the altitude of side lobes occurring due to the surface wave diffraction at the boundaries of the antenna substrate.

The 2D PhC design is done by creating holes in a suitable substrate. In 2D-PhC, there are two types of lattice shapes, triangles and squares. This paper adopts the square lattice arrangement for the design of the PhC structure; these square lattices impose restrictions on the propagation

of electromagnetic waves. They lessen the return loss and enhance the gain with the partitioning of $2\pi/a$ with the Brillouin zone. Figure 1 shows the PBG structure of the proposed antenna. The band gap structure helps to calculate the normalized frequency of the antenna. Normalized frequency is a/λ and the gap in the mid-gap frequency ratio is $\Delta\omega/\omega$. The normalized frequency range of the I-shaped antenna is $0.648–0.665 a/\lambda$. The band structure depends on the value of the ratio r/a , where r is the radius of the air-hole and a is the lattice parameter. The band gap swings to advanced frequency ranges as the hole radii eases, and the transmission coefficient decreases associated with the increase of hole radius.

Proposed Design

The proposed work is the design of the TMPA array using PhC substrate. The antenna substrate uses Rogers RO4350; it offers great features such as excellent electrical properties, high-frequency performance and enhanced gain. The dielectric constant is 3.48 and the loss tangent value is 0.004. because of the presence of a surface wave, the design of conventional 2×1 TMPA (Antenna1) expels more power loss and less gain. The design of the PhC antenna uses the same conventional antenna configuration. It comprises five different-shaped holes such as L, H, I, T, and inverted L holes in the PhC substrate. The CST software simulates the proposed antenna structures. The influence of various air-hole PhC substrates is analyzed and compared with conventional TMPA arrays.

Conventional Antenna

Figure 2 shows the proposed model of conventional TMPA. In the arrangement of the TMPA array, the length and width

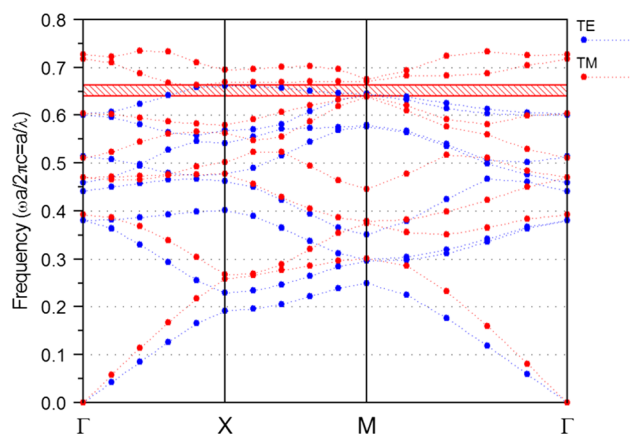


Fig. 1 PBG range of proposed antenna structure

of the ground are $27.8 \times 25.4 \mu\text{m}^2$. The substrate follows the exact dimension as the ground. For the ground, the patch and the feed, copper material is used for its high electrical and good corrosion resistance. The antenna dimensions are calculated^{22,23} using the resonating frequency (f_r). Hence, f_r can be written as

$$f_r = \frac{2c}{3x\sqrt{\epsilon_r}} \tag{1}$$

where ‘ c ’ is the light speed in vacuum, ‘ f_r ’ is antenna resonant frequency, ‘ ϵ_r ’ is the relative permittivity of the substrate and ‘ x ’ is a side of the trigonal patch (let $x = L_3 = L_4$).

The trigonal side ‘ a ’ can be obtained from the following equation,

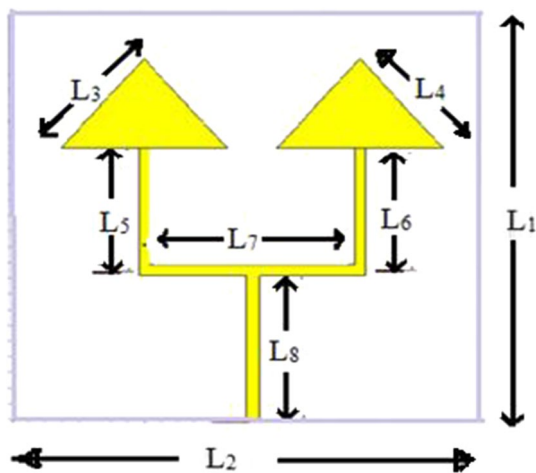


Fig. 2 Structure of conventional antenna design (Antenna 1)

$$x = \frac{2c}{3f_r\sqrt{\epsilon_r}} \tag{2}$$

In Fig. 2, the value of L_1 is $25.4 \mu\text{m}$, L_2 is $27.8 \mu\text{m}$, L_3 and L_4 are $7 \mu\text{m}$, L_5 and L_6 are $8 \mu\text{m}$, L_7 is $12.9 \mu\text{m}$ and L_8 is $9 \mu\text{m}$. The proposed conventional antenna (Antenna 1) resonates at the frequency of 8.98 THz with a return loss -32.97 dB . The obtained value of VSWR is 1.045 , the gain of the conventional antenna is 1.954 dB and the directivity is 3.22 dBi .

PhC Antenna Using L-Shaped Hole Structure

The PhC substrate can reduce the power loss and raise the gain compared with the conventional antenna. Different shapes are used to drill holes into the substrate materials, such as circles, squares, and hexagons. Instead of using a circular air hole in the PhC substrate, the proposed antennas are designed with T, L, H, I and inverted L air holes. In this section, the trigonal patch antenna is placed on the topmost surface of the PhC substrate with L-shaped holes. The L-shaped ($1.5 \times 1.5 \mu\text{m}^2$) air columns are punched into the square lattice PhC substrate. This PhC substrate consists of 4×5 arrays of L-shaped holes in the Rogers slab, as shown in Fig. 3. In patch antenna design, the substrate height plays a vital role; hence it is necessary to find the effective ‘ h ’ value. The height of the PhC substrate is varied for different ‘ h ’ values and the antenna performances are analyzed, which is shown in Table I. Based on the output characteristics of various antennas, the optimal value is found as $3 \mu\text{m}$. This particular L-shaped PhC structure helps to control the light flow and decreases signal loss. The influence of L-holes PhC structure improves

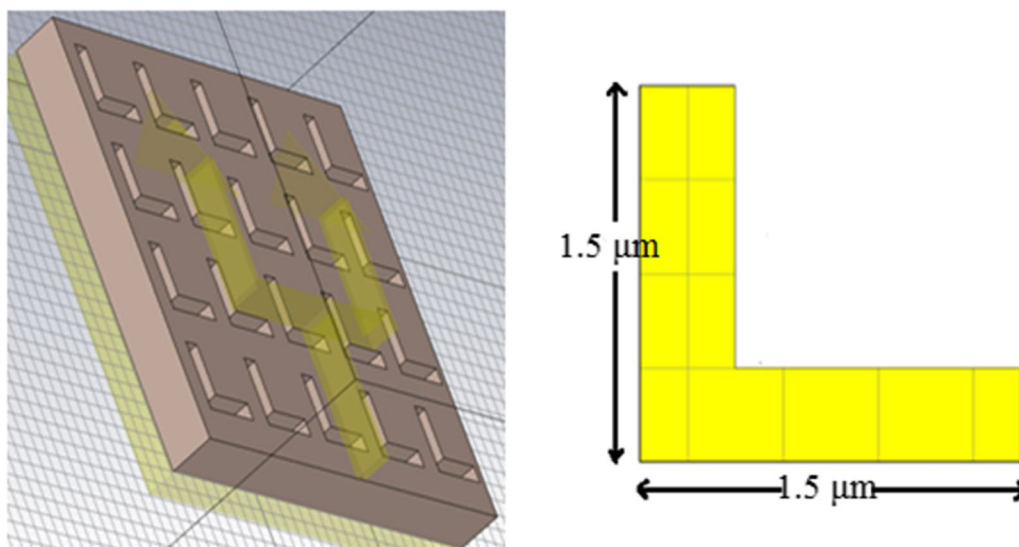


Fig. 3 L Shaped PhC substrate structure (Antenna 2)

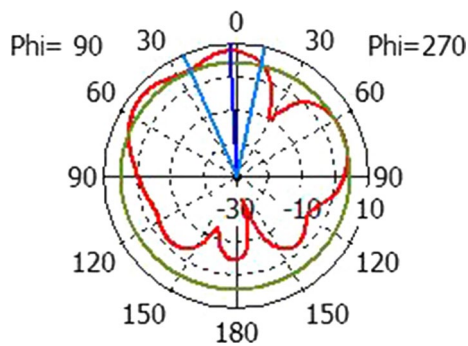


Fig. 4 Radiation pattern of L shaped PhC Structure

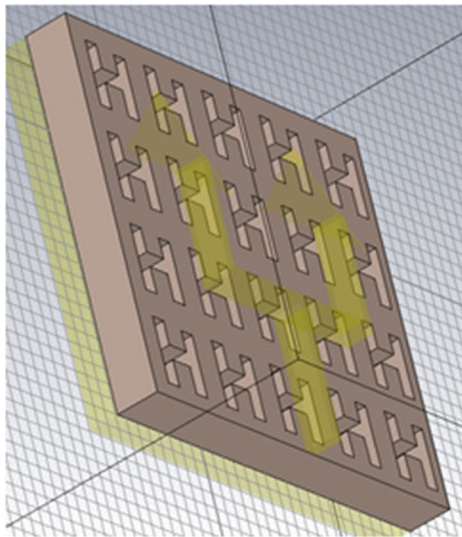


Fig. 5 H-shaped PhC substrate structure (Antenna 3)

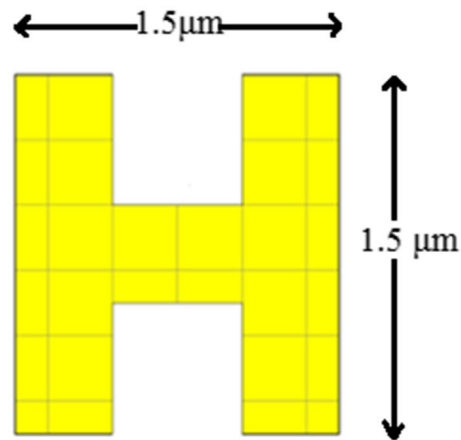
Table I Impact of various ‘*h*’ values of the L-shaped PhC structure

‘ <i>h</i> ’ values in μm	Freq. in THz	Return loss in dB	VSWR	Gain in dB	Directivity in dBi
1	14.28	- 11.87	1.68	2.75	2.12
3	9.74	- 41.05	1.01	5.67	7.70
5	4.21	- 18.44	1.27	1.56	1.96
7	1.91	- 7.59	2.43	2.34	2.54
9	1.87	- 10.16	1.89	1.16	3.53
11	1.77	- 12.72	1.60	3.81	2.89

the return loss of -41.05 dB at a resonant frequency of 9.74 THz. Figure 4 illustrates the radiation pattern of this structure. The maximum radiation was obtained at the angle of both 0° and 60° with a good directivity of 8 dBi. Due to the suppression of the surface wave by PhC substrate, the major power radiation occurs in the air-side.

The VSWR obtained for this structure is 1.017 , which is near unity. Also, the PBG structure increased the gain of the L-shaped PhC structure is 5.67 dB. The energy of the electric field absorbed by the traditional antenna from surface waves is, of course, more than most of that consumed by the PBG antenna. As a result of PBG, the accumulation of electromagnetic waves by the substrate is decreased and their energy is replicated in the open space so that the gain and return loss are greatly amended.^{20,24–26}

PhC Antenna Using H-Shaped Hole Structure



This PBG structured TMPA (Antenna 3) is designed with 4×5 small H-shaped holes ($1.5 \times 1.5 \mu\text{m}^2$) in Rogers substrate material and is shown in Fig. 5. This PhC structure acts as a reflective wall to disrupt the surface wave. It also supports obtaining the minimal return loss value -42.16 dB at 10.21 THz over an L-shaped PhC antenna. The VSWR of this structure is 1.015 around unity. From the simulation, the output gain and the directivity of small H-shaped PhC are 8.3 dB and 7.5 dBi. The radiation plot of this structure is shown in Fig. 6. The major lobe has a maximum peak at the angle of 0° , which increases the antenna directivity. The minimum power radiates in the PhC substrate bottom, whereas it is less than that of the power radiated from the top face of the substrate. Further, the design involves different antennas by altering the substrate height value. Table II lists the performances of these antennas. It shows the output characteristics of different ‘*h*’ values of the patch antenna. It is observed that the proposed antenna performance is good for the structure with an ‘*h*’ value of $3 \mu\text{m}$ and this structure is considered an ideal one.

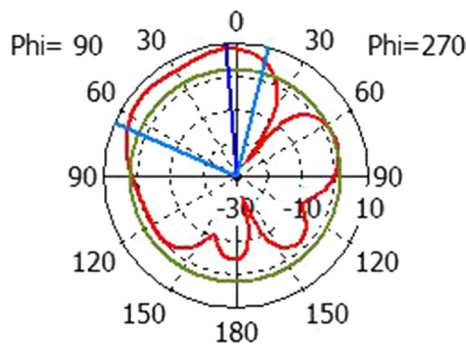


Fig. 6 Radiation plot of H-shaped PhC antenna

The minimal return loss value -55.84 dB at 9.66 THz is attained and it is better than the H-shaped PhC antenna. Figure 8 shows the radiation pattern of the T-shaped air hole structure. The major power radiates towards the air side of the substrate between the angle of 0° to 30° . The VSWR of this structure is 1.003 around unity and the directivity is 7.55 dBi. The gain of the T-shaped PhC antenna is acquired in the value of 5.5 dB. The discussed output parameters are obtained from the structure with substrate height ' h ' of $3 \mu\text{m}$. Also, various patch antennas are designed and simulated for different ' h ' values and the analysis is made. Table III shows the various antenna performances for different structures. It is concluded that

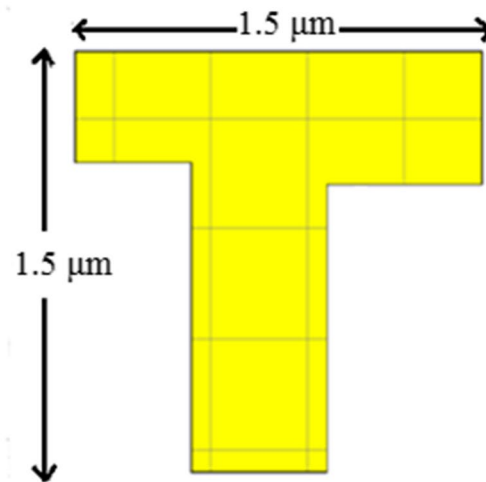
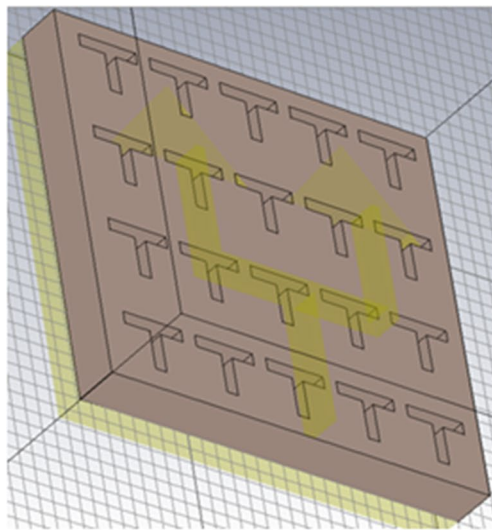


Fig. 7 Trigonal PhC patch antenna structure (Antenna 4) with a T-shaped hole

Table II Effect of various ' h ' values of H-shaped PhC structure

' h ' values in μm	Freq. in THz	Return loss in dB	VSWR	Gain in dB	Directivity in dBi
1	4.79	-15.19	1.42	1.72	2.09
3	10.21	-42.16	1.01	7.50	8.30
5	4.40	-17.88	1.29	2.58	3.94
7	2.04	-7.92	2.34	1.45	2.58
9	1.98	-10.84	1.80	3.74	1.57
11	1.87	-15.30	1.41	2.87	2.87

PhC Antenna Using T-Shaped Hole Structure

The T-shaped holes in the PhC structure are designed by considering Rogers as a substrate material. Figure 7 shows the PhC substrate comprising a 4×5 array of T-shaped structures ($1.5 \times 1.5 \mu\text{m}^2$) in the antenna model.

$h = 3 \mu\text{m}$ exhibits better antenna characteristics than the other values.

PhC Antenna Using Inverted L-Shaped Hole Structure

This structure was designed as an inverted L-shaped structure, as shown in Fig. 9. This PhC substrate comprises 4×5 inverted L air holes ($1.5 \times 1.5 \mu\text{m}^2$) and it helps to increase the antenna performances. The various inverted L-shaped PhC antennas are designed for different substrate heights. The ' h ' values vary between $1 \mu\text{m}$ and $11 \mu\text{m}$. The output of various structures is analyzed, and Table IV shows the output. Based on the output characteristics of various antenna structures, the best ' h ' value is $3 \mu\text{m}$. The S11 parameter of this structure is -58.51 dB; it is a lot less than the other ' h ' value antennas. Other exclusive antenna parameters such as gain and VSWR are 6.5 dB at 9.77 THz and 1.002 . Figure 10 shows the radiation plot of this antenna. It is observed that

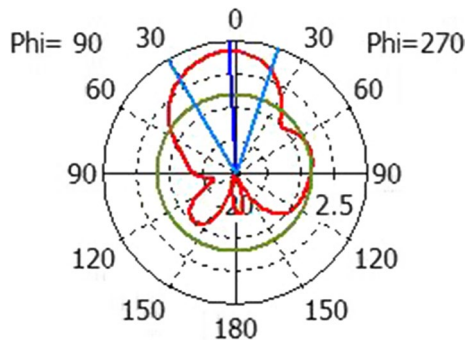


Fig. 8 Radiation pattern of a T-shaped PhC antenna

Table III Consequence of various ‘*h*’ values of T-shaped PhC structure

‘ <i>h</i> ’ values in μm	Freq. in THz	Return loss in dB	VSWR	Gain in dB	Directivity in dBi
1	14.28	– 26.04	1.10	2.63	1.95
3	9.66	– 55.84	1.00	5.55	7.55
5	4.04	– 12.62	1.61	3.48	4.89
7	1.89	– 7.69	2.40	2.29	3.56
9	1.85	– 10.05	1.91	2.50	4.53
11	1.77	– 13.09	1.56	1.71	3.55

the main lobe is at an angle of 65° with a magnitude of 8 dBi. The maximum directivity is obtained in the upper face of PhC and the directivity at the bottom face is significantly less.

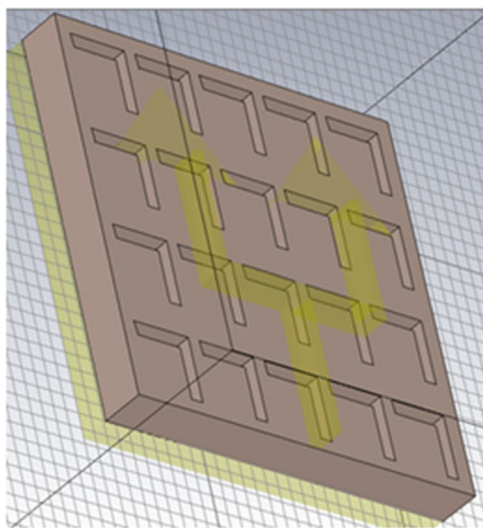


Fig. 9 Inverted L-shaped PhC substrate structure (Antenna 5)

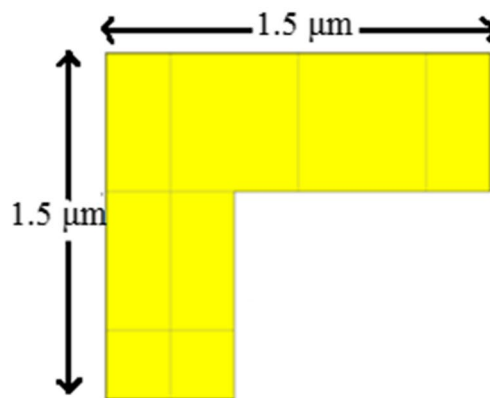
PhC Antenna Using I-Shaped Hole Structure

This design shows the antenna with the I-shaped structure. Figure 11 shows the antenna designed with the I-shaped air hole ($1.5 \times 0.8 \mu\text{m}^2$) PhC antenna helps decrease the surface waves. It provides good return loss, improved gain, and directivity compared with the antenna structures mentioned above. The proposed THz TMPA offers the minimum return loss of -58.99 dB at $h = 3 \mu\text{m}$. The remaining ‘*h*’ values of antenna structures exhibit poor performances as shown in Table V. Hence, the antenna with a substrate height of $3 \mu\text{m}$ is proven to be the ideal value. The obtained voltage standing wave ratio is 1.002 at 9.3 THz. Figure 12 illustrates that the large main lobe occurs in between angles of 0° and 90° . With the influence of radiation mode, the I-shaped PhC antenna exhibits a power more significant than the other structures. The gain and directivity of the I-shaped antenna are obtained as 9.1 dB and 10.7 dBi.

Discussion of Simulated Result

Detailed Analysis of Different Proposed Antenna Works

Table VI denotes the entire performance of all the six proposed structures, which are operating in the THz frequency with all the required parameters. There is more signal loss in the traditional TMPA due to surface waves and -32.97 dB return loss is achieved. The table explains the characteristics of various PhC antenna models. A PhC antenna has better output than the conventional one, and Fig. 13 illustrates the



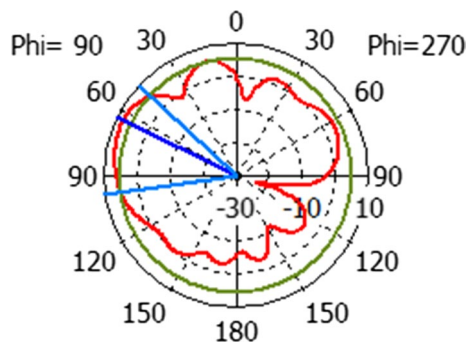


Fig. 10 Radiation characteristics of inverted L-shaped PhC antenna

Table IV Consequence of various ‘h’ values of inverted L-shaped PhC structure

‘h’ values in μm	Freq. in THz	Return loss in dB	VSWR	Gain in dB	Directivity in dBi
1	13.88	- 13.8	1.02	2.70	2.03
3	9.77	- 58.51	1.00	6.59	8.00
5	4.11	- 14.64	1.45	1.53	3.93
7	1.87	- 7.65	2.41	3.27	2.54
9	1.87	- 9.19	2.06	2.59	4.53
11	1.77	- 11.78	1.77	1.75	1.53

S11 parameter. Because of the arrangement on a dielectric substrate, the PBG act as a stopband of electromagnetic waves. The PhC substrate antenna designs give minimal

return loss, wider bandwidth, and high gain; hence, radiating energy coupling increases in free space.

The table clearly shows the various comparisons for the different parameters of the antenna. The excellent return loss has been obtained from the I-shaped PhC structure (Antenna 6). It concludes that Antenna 6 provides better directivity and gain at an operating frequency of 9.3 THz. The characteristics of the proposed structures’ electromagnetic transmission are drastically enhanced due to the PhC substrate’s contact.²⁷ The PhC informs the substrate frequency and directional selectivity that are standout in the microwave field. The stopband of the PhC rejects most of the intensity emanated by an antenna anchored on its layer in the absence of shorting out the driving-point impedance. As for radiation magnitude, the microstrip patch antenna on the I-shaped PhC structure exhibited a gain value 4.7 times more than that of the conventional TMPA. It is observed that the impact of a slight discrepancy from the collinearity of the conventional patch antenna. Most of the radiation dispersed from the dielectric substrate commits oneself to the forward planisphere. For the photonic crystal substrate, polar plots having an indistinguishable eccentric scale that increases gain and lower return loss.

Ameliorating the Lattice Value (a) of I-Shaped Hole PhC Structure

This section investigates the antenna structures by mutating the multiple spacing values ‘a’ between the holes from 1 to 10 μm . Table VII shows the obtained antenna characteristics

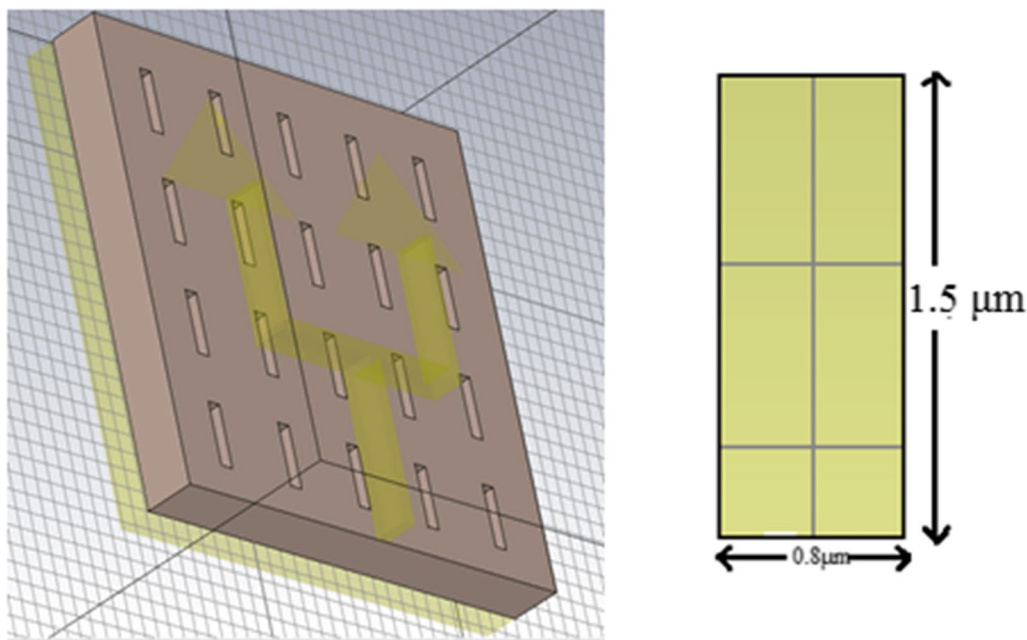


Fig. 11 I-shaped PhC substrate structure (Antenna 6)

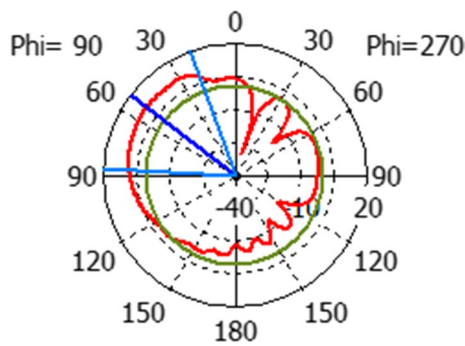


Fig. 12 Radiation characteristics of the I-shaped PhC antenna

from the various lattice values. The table also shows the impact of the return loss of different lattices values. At $a = 5.2 \mu\text{m}$, the antenna exhibits excellent features such as -58.99 dB return loss at 9.3 THz with a bandwidth of 0.93 THz and proves that it is the optimum value compared to the others. The consequence of modifications in the lattice constant 'a' was investigated and antenna performances are enhanced in 2D PhC. The lattice constant plays a vital role in the structural parameter that determines the enhancement ratio of antenna efficiency. When the lattice value changes, a shift occurs in the operating frequency. The impact of the overlapped electric field leads to changes in the refractive index. Hence, the refractive index variations into the air holes result in a shift in the frequency band.^{28,29}

Comparison of the Proposed Antenna Design with Prevailing Works

The entire antenna features of the proposed structure are compared with the prevailing structures, as illustrated in Table VIII. Anand et al.^{6,15} proposed a THz antenna with PBG substrate and obtained the gain value around 5 dB for the frequency of 0.75 THz and 2.15 THz . Tripathi et al.^{8,13} designed the PBG antenna, which resonates at a frequency of 1.04 THz and 0.69 THz with a gain of 7.99 dB and 5.74 dB . Shahid et al.¹⁶ investigated the THz antenna with PBG material which produces 6.88 dB gain at 0.69 THz . Ritesh et al.²⁰ proposed a PBG antenna that gave the value of return loss

and gain of -44.71 dB and 7.9 dB . Vahdati et al.³⁰ studied a PBG antenna structure that produced a gain of 7.7 dB . Britto et al.³² studied a PhC antenna with a triangular lattice structure and obtained -57.81 dB at 2.37 THz . Amarveer et al.³³ designed a PhC antenna PBG and obtained a gain and directivity of around 5 dB at 0.67 THz . The above-mentioned existing research works examined only the standard circular air hole PhC structure. Hence, the proposed antenna with the unique air hole produces the best output and it is more efficient than the regular PhC pattern with circular holes.

Conclusion

This paper analyzed the 2D PhC antenna operating in the THz frequency. The proposed PhC antenna utilizes various air hole shapes such as T, L, H, I and inverted L. These structures are simulated and the antenna characteristics are contrasted. When an L-shaped hole is introduced on the PhC substrate, it produced a return loss of -41.46 dB , which is low compared with the conventional antenna return loss of -32.97 dB . Further, the return loss values of other shapes

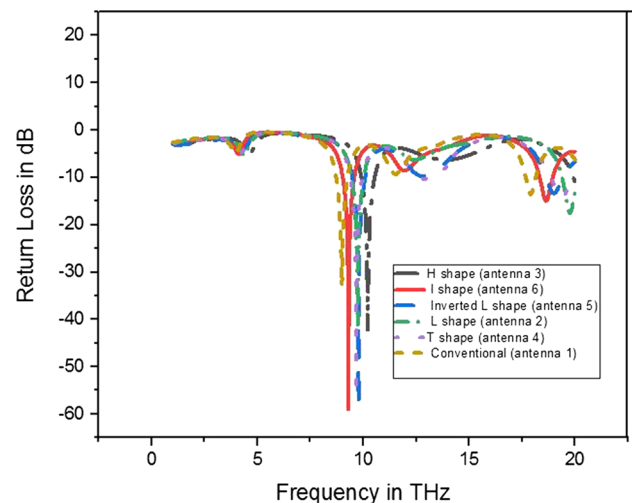


Fig. 13 Frequency versus return loss for various simulated antenna structures

Table V Result of various 'h' values of I shaped PhC structure

'h' values in μm	Freq. in THz	Return loss in dB	VSWR	Gain in dB	Directivity in dBi
1	13.82	-16.72	1.34	1.66	3.99
3	9.30	-58.99	1.00	9.10	10.78
5	3.92	-13.68	1.52	1.51	2.94
7	1.83	-7.44	2.48	1.29	1.65
9	1.79	-8.85	2.12	1.53	2.52
11	1.72	-10.36	1.87	1.76	1.53

Table VI Comparison of five different antennas with conventional antenna parameters

Proposed antennas	Antenna parameters					
	f_r in THz	Return loss in dB	VSWR	Directivity in dBi	Gain in dB	Bandwidth in THz
Antenna 1 (TMPA)	8.98	- 32.97	1.045	3.22	1.95	0.78
Antenna 2 (L-shaped)	9.74	- 41.05	1.017	7.7	5.67	1.24
Antenna 3 (H-shaped)	10.21	- 42.16	1.015	8.3	7.5	1.41
Antenna 4 (T-shaped)	9.66	- 55.84	1.003	7.5	5.5	0.57
Antenna 5 (Inverted L-shaped)	9.77	- 58.51	1.002	8	6.5	0.61
Antenna 6 (I-shaped)	9.30	- 58.99	1.002	10.7	9.1	0.54

Table VII Impact of various lattice values in I hole structure

Lattice constant value 'a' in μm	Antenna parameters					
	F_r in THz	Return loss in dB	VSWR	Directivity in dBi	Gain in dB	Bandwidth in THz
1	9.56	- 22.31	1.113	3.58	2.48	0.51
2	9.74	- 26.13	1.103	3.76	2.34	0.53
3	9.47	- 33.24	1.044	3.59	2.20	0.74
4	9.37	- 38.16	1.025	3.49	2.14	0.90
5	9.24	- 44.47	1.012	3.50	2.17	0.90
5.2	9.30	- 58.99	1.002	10.7	9.1	0.93
5.4	9.34	- 25.65	1.110	3.43	2.14	0.92
5.6	9.36	- 24.95	1.119	3.34	2.09	0.88
5.8	9.39	- 25.30	1.114	3.42	2.14	0.70
6	9.34	- 37.62	1.026	3.46	2.14	0.90
7	9.03	- 27.94	1.083	3.30	2.01	1.2
8	9.03	- 29.88	1.066	3.25	1.98	1.3
9	9.17	- 27.56	1.087	3.44	2.07	0.9
10	9.15	- 30.07	1.064	3.43	2.08	0.6

Table VIII Comparison of proposed antenna characteristics with existing structures

Existing works references	Antenna characteristics				
	Frequency (THz)	Return loss (dB)	Gain (dB)	Directivity (dBi)	VSWR
Proposed PhC Structure [Antenna 6]	9.3	- 58.99	9.1	10.7	1.002
Anand et al. ⁶	0.75	-	5.09	5.71	-
Tripathi et al. ⁸	1.04	-	7.99	8.42	-
Anand et al. ¹⁵	2.15	< - 15	4.97	-	-
Shahid et al. ¹⁶	0.69	- 34.9	6.88	7.01	1.043
Ritesh et al. ²⁰	0.63	- 44.71	7.94	8.61	1.011
Vahdati et al. ³⁰	1.4	- 28.5	7.7	-	-
Tripathi et al. ³¹	0.69	-	5.74	6.57	-
Britto et al. ³²	2.37	- 57.81	9.2	-	1.002
Amarveer et al. ³³	0.67	-	5.22	5	-

such as H, T and inverted L PhC antenna has reduced to - 42.16 dB, 55.84 dB and - 58.51 dB. Finally, the optimum value of return loss - 58.99 dB is obtained from the

I-shaped hole antenna. The gain of the conventional antenna is 1.04 dB, whereas the PhC antenna obtains gain up to a value of 9.1 dB with a directivity of 10.7 dBi. The structure

of the antenna is small in size, so that it consumes only a small amount of power. This proposed PhC antenna structure supports high-speed data rate wireless systems, automotive radar sensors, and aircraft register.

Conflict of interest The authors declare that there are no conflicts of interest related to this article.

References

1. J.F. O'Hara, S. Ekin, W. Choi, and I. Song, *Technologies* 7, 43 (2019).
2. I. Malhotra, K.R. Jha, and G. Singh, *Int. J. Microw. Wirel. Technol.* 10, 271 (2018).
3. T. Robin, C. Bouye, and J. Cochard, Terahertz applications: trends and challenges. in Proc. SPIE 8985, Terahertz, RF, Millimeter, and Submillimeter-Wave Technology and Applications VII, 898512 (2014). <https://doi.org/10.1117/12.2043284>
4. H. Davoudabadifarahani, and B. Ghalamkari, *Optik* 194, 163118 (2019).
5. G. Singh, *Infrared Phys. Technol.* 53, 17 (2010).
6. S. Anand, D. Sriram Kumar, R.J. Wu, and M. Chavali, *Optik* 125, 5546 (2014).
7. E. Fritz-Andrade, H. Jardon-Aguilar, and J.A. Tirado-Mendez, *Radioengineering* 27, 976 (2019).
8. S.K. Tripathi, and A. Kumar, *Austral. J. Electr. Electron. Eng.* 16, 74–80 (2019).
9. D.R. Smith, J.B. Pendry, and M.C.K. Wiltshire, *Science* 305, 788 (2004).
10. D.A. Pawlak, *Sci. Plena* 4 (2008). <https://www.semanticscholar.org/paper/Metamaterials-and-photonic-crystals-%E2%80%93-potential-for-Pawlak/ab84a947f54c71cb1894de86cfb87b0efc5c689e# citing-papers>.
11. M.V. Rybin, D.S. Filonov, K.B. Samusev, P.A. Belov, Y.S. Kivshar, and M.F. Limonov, Transition from photonic crystals to dielectric metamaterials: a phase diagram and the order parameter. in Proc. SPIE 9885, Photonic Crystal Materials and Devices XII, 98850R, (2016).
12. V.M. Shalaev, W. Cai, U.K. Chettiar, H.-K. Yuan, A.K. Sarychev, V.P. Drachev, and A.V. Kildishev, *Opt. Lett.* 30, 3356 (2005).
13. P. Moitra, Y. Yang, Z. Anderson, I.I. Kravchenko, D.P. Briggs, and J. Valentine, *Nature Photon* 7, 791–795 (2013).
14. S. Kumar Danasegaran, E.C. Britto, and W. Johnson, *Opt. Eng.* 59, 087102 (2020).
15. S. Anand, D.S. Kumar, R. Wu, and M. Chavali, *Optik* 125, 2835 (2014).
16. S. Ullah, C. Ruan, T. Ul Haq, and X. Zhang, *J. Electromagn. Waves Appl.* (2019). <https://doi.org/10.1080/09205071.2019.1654929>.
17. J.D. Joannopoulos, S.G. Johnson, J.N. Winn, and R.D. Meade, *Photonic crystals—molding the flow of light*, 2nd ed., (New Jersey: Princeton University Press, 2008).
18. R. Kumar Kushwaha, and P. Karuppanan, *Microwave Opt. Technol. Lett.* 62, 439 (2019).
19. M.S. Rabbani, and H. Ghafouri-Shiraz, *Microw. Opt. Technol. Lett.* (2017). [https://doi.org/10.1002/mop.30332.59.3.\(511-514\)](https://doi.org/10.1002/mop.30332.59.3.(511-514)).
20. R.K. Kushwaha, P. Karuppanan, and L.D. Malviya, *Phys. B Condens. Matter* 545, 107 (2018).
21. D. S. Kumar, P. Prithika and B. E. Caroline, Investigating the performance of microstrip patch antenna with photonic crystal on different substrate. in IEEE International Conference on System, Computation, Automation and Networking, (2019), pp. 1-5,
22. A.C. Lepage, X. Begaud, G. Le Ray, and A. Sharaiha, *Int. J. Antennas Propag.* (2008). <https://doi.org/10.1155/2008/410786>.
23. D.S. Kumar, B.E. Caroline, and S. Thilagavathi, Investigation of equilateral triangular microstrip patch antenna using photonic crystal. in International Conference on System, Computation, Automation and Networking, pp. 1–6, (2020)
24. Z. Li, Y.L. Xue, and T. Shen, *Math. Probl. Eng.* 2012, 151603 (2012).
25. A. Nejati, R.A. Sadeghzadeh, and F. Geran, *Phys. B Condens. Matter* 449, 113 (2014).
26. J.P.P. Pereira, J.P. da Silva, and H.D. de Andrade, *Microw. Opt. Technol. Lett.* 57, 2147 (2015).
27. E.R. Brown, C.D. Parker, and E. Yablonovitch, *J. Opt. Soc. Am. B* 10, 404 (1993).
28. H.-S. Kitzrow, H. Matthias, S.L. Schweizer, H.M. van Driel, and R.B. Wehrspohn, *Adv. Opt. Technol.* 2008, 780784 (2008).
29. J.R. Oh, Y.K. Lee, H.K. Park, and Y.R. Do, *J. Appl. Phys.* 105, 043103 (2009).
30. A. Vahdati, and F. Parandin, *Wirel. Pers Commun.* 109, 2213 (2019).
31. S.K. Tripathi, and A. Kumar, *Manag. J. Commun. Eng. Syst.* 6, 16 (2017).
32. E.C. Britto, S.K. Danasegaran, and W. Johnson, *Int. J. Commun. Syst.* 34, e4662 (2021). <https://doi.org/10.1002/dac.4662>.
33. Amarveer Singh Dhillon, A.S. Dhillon, D. Mittal, and E. Sidhu, *Optik* 144, 634 (2017).

Publisher's Note Springer Nature remains neutral with regard to jurisdictional claims in published maps and institutional affiliations.